Author for correspondence:
Dr Ahmed Abdel Khalek Abdel Razek,
Department of Diagnostic Radiology,
Mansoura University Faculty of Medicine,
Elgomheryia Street, Mansoura, Egypt 3512
E-mail: arazek@mans.edu.eg
Fax: +20 502 259 146

Prediction of skull base osteomyelitis in necrotising otitis externa with diffusion-weighted imaging

A A K Abdel Razek and W Mahmoud

Department of Diagnostic Radiology, Mansoura University Faculty of Medicine, Mansoura, Egypt

Abstract

Objective. To predict skull base osteomyelitis in patients with necrotising otitis externa using diffusion-weighted imaging.

Methods. A retrospective analysis was conducted of 25 necrotising otitis externa patients with skull base osteomyelitis ($n = 10$) or without skull base involvement ($n = 14$) who underwent a single-shot diffusion-weighted imaging of the skull base.

Results. The respective mean apparent diffusion coefficient values of the skull base, as determined by two reviewers, were 0.851 ± 0.15 and $0.841 \pm 0.14 \times 10^{-3}$mm^2/s for the skull base osteomyelitis patients, and 1.065 ± 0.19 and $1.045 \pm 0.20 \times 10^{-3}$mm^2/s for the necrotising otitis externa patients without skull base involvement. The difference in apparent diffusion coefficients between the groups was significant, for both reviewers ($p = 0.008$ and 0.012). The optimal threshold apparent diffusion coefficient for predicting skull base osteomyelitis in necrotising otitis externa patients was 0.945×10^{-3}mm^2/s and 0.915×10^{-3}mm^2/s, with an area under the curve of 0.825 and 0.800, accuracy of 87.5 and 83.3 per cent, sensitivity of 85.7 and 90.0 per cent, and specificity of 90.0 and 78.6 per cent, for each reviewer respectively.

Conclusion. Apparent diffusion coefficient is a non-invasive imaging parameter useful for predicting skull base osteomyelitis in necrotising otitis externa patients.

Introduction

Necrotising otitis externa is an invasive infectious process of the external auditory canal that may extend into the skull base.[1–3] Skull base osteomyelitis is a rare but serious and life-threatening complication that is mostly secondary to necrotising otitis externa. The mortality rate of skull base osteomyelitis is 33 per cent, reaching up to 80 per cent in patients with cranial nerve involvement.[4–8] The management for patients with skull base osteomyelitis is different from that for patients with necrotising otitis externa without skull base involvement. Surgery may be used in the treatment of skull base osteomyelitis, especially when there is cranial nerve involvement.[7–9]

Imaging is used for the assessment of skull base osteomyelitis, but the results overlapping with imaging findings for necrotising otitis externa.[10–12] Routine magnetic resonance imaging (MRI) and isotope studies are used for the prediction of skull base osteomyelitis, but their results are non-specific.[13–15] Diffusion-weighted imaging offers better characterisation of the soft tissues and their physiological processes because it reflects the random motion of the water protons, which is disturbed by the intracellular organelles and macromolecules located within the tissues.[16,17] Diffusion-weighted imaging is commonly used for the assessment of head and neck cancer,[17,18] soft tissue infection,[19,20] and bone infection with osteomyelitis.[21–23] It is commonly used in the assessment of middle-ear cholesteatoma and recently in the characterisation of external-ear masses.[24,25]

Only one study has discussed the role of diffusion-weighted imaging in the follow up of patients with necrotising otitis externa.[26] To our knowledge, no previous study in the English literature has investigated the role of diffusion-weighted imaging for predicting skull base osteomyelitis in necrotising otitis externa patients. This work aimed to predict skull base osteomyelitis in patients with necrotising otitis externa using diffusion-weighted imaging.

Materials and methods

Patients

This study was approved by the ethics board; the need for patients' informed consent was waived given that this is a retrospective study. A retrospective analysis was conducted of the magnetic resonance images of patients with necrotising otitis externa. The inclusion criteria were patients with necrotising otitis externa who underwent diffusion-weighted imaging. We excluded only one patient from the study, because of motion artefacts.

A total of 24 patients were included in this study (18 males and 6 females), with a mean age of 53 years (age range, 44–62 years). These patients presented with: external-ear

swelling ($n = 24$), headache ($n = 24$), otalgia ($n = 24$), otorrhoea ($n = 19$), trismus ($n = 18$) and cranial nerve palsy ($n = 8$). All patients were diabetic and the final diagnosis was confirmed via biopsy. Patients were classified according to skull base involvement and spilt into two groups accordingly: necrotising otitis externa without skull base involvement ($n = 14$), or necrotising otitis externa with skull base osteomyelitis ($n = 10$).

Routine magnetic resonance imaging

Magnetic resonance imaging of the petrous bone was performed on a 1.5 Tesla Symphony scanner (Siemens, Munich, Germany) using a head coil with a circular polarised surface. All patients underwent axial T1-weighted imaging (repetition time = 800 ms, echo time = 15 ms) and axial T2-weighted imaging (repetition time = 800 ms, echo time = 20 ms), with section thickness of 3 mm, an interslice gap of 1–2 mm, and field of view of 25×20 cm. Axial, contrast-enhanced, T1-weighted images (repetition time = 800 ms, echo time = 15 ms) were obtained after an intravenous bolus injection of gadopentetate gadolinium (0.1 ml/kg of body weight).

Diffusion-weighted imaging

A single-shot echo-planar imaging diffusion-weighted imaging ('EPI-DWI') sequence was used prior to contrast medium injection with b-values of 0, 500 and 1000 s/mm^2. The imaging parameters were: repetition time = 1000 ms, echo time = 108 ms, field of view = 25×20 cm and section thickness = 5 mm, with an interslice gap of 1–2 mm. The apparent diffusion coefficient map was automatically constructed.

Image analysis

Image analysis was performed by two radiologists (AA and WM) with 30 and 11 years' respective experience in head and neck imaging. They independently calculated the apparent diffusion coefficient of the skull base lesion; the radiologists were blinded to the patient data and the final diagnosis. A region of interest was drawn on the apparent diffusion coefficient map using an electronic cursor at the skull base lesion, and the apparent diffusion coefficient value of the lesion was calculated.

Statistical analysis

The data were described in terms of mean and standard deviation values. The data were analysed to determine statistically significant differences. The student's t-test was used to compare the two groups (necrotising otitis externa patients with or without skull base involvement). The p-value was considered significant if 0.05 or lower. Receiver operating characteristic curves were used to determine the optimal threshold apparent diffusion coefficient for predicting skull base osteomyelitis in patients with necrotising otitis externa. The data were statistically analysed using SPSS software version 22 (SPSS, Chicago, Illinois, USA).

Results

All patients with suspected skull base osteomyelitis presented with otalgia and otorrhoea; 34 per cent had cranial nerve palsies and 17 per cent had hearing loss. Culture was positive for *Pseudomonas aeruginosa* in 12 patients (50 per cent).
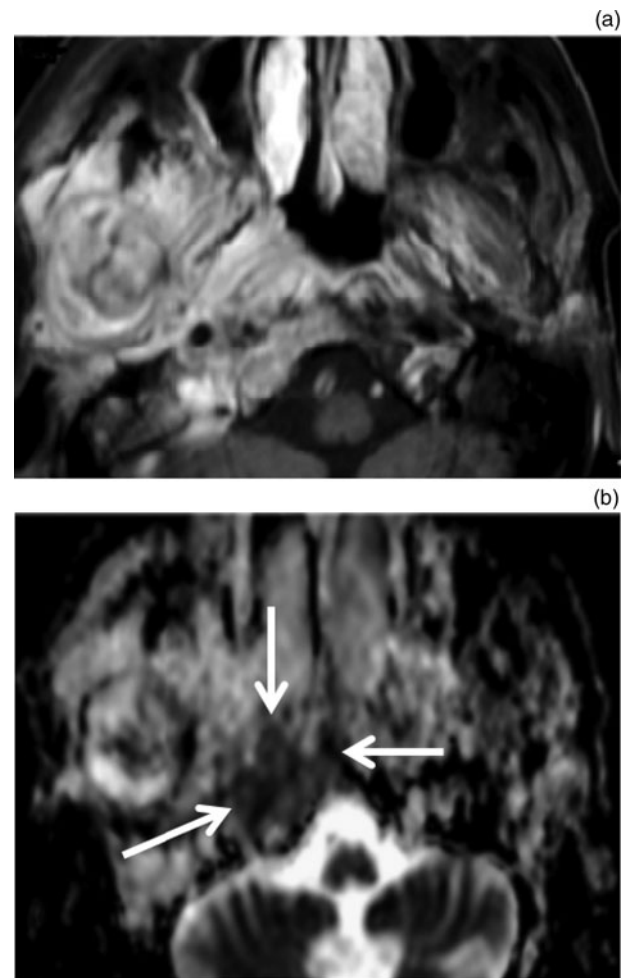

Fig. 1. Necrotising otitis externa with skull base osteomyelitis. (a) Axial, contrast-enhanced magnetic resonance imaging scan shows diffuse enhancing lesion infiltrating the right masticator space in a patient with necrotising otitis externa. The lesion extends into the skull base bone marrow on the right side. Note abnormal marrow signal intensity of the ramus of the right mandible, denoting osteomyelitis of the mandible. (b) Apparent diffusion coefficient map shows low apparent diffusion coefficient values for the bony lesion of the skull base (arrows), with calculated apparent diffusion coefficient values of 0.83 and 0.79 $\times 10^{-3}$ mm^2/s for each reviewer respectively.

Staphylococcus aureus was the causative organism in 8 patients (34 per cent). Fungal infection was found in two patients. The causative organism was difficult to detect in two patients in light of antibiotics given prior to MRI.

The mean apparent diffusion coefficient of the skull base in patients with skull base osteomyelitis ($n = 10$) (Figure 1) was $0.851 \pm 0.15 \times 10^{-3}$ mm^2/s (range, 0.72–1.23×10^{-3} mm^2/s) for the first reviewer and $0.841 \pm 0.14 \times 10^{-3}$ mm^2/s (range, 0.74–1.20) for the second reviewer (Table 1). The mean apparent diffusion coefficient of the skull base in patients with necrotising otitis externa without skull base involvement ($n = 14$) (Figure 2) was $1.065 \pm 0.19 \times 10^{-3}$ mm^2/s (range, 0.73–1.32×10^{-3} mm^2/s) for the first reviewer and $1.045 \pm 0.20 \times 10^{-3}$ mm^2/s (range, 0.73–1.30×10^{-3} mm^2/s) for the second reviewer. There was a significant difference in the apparent diffusion coefficient of the skull base between necrotising otitis externa patients with and without skull base osteomyelitis for the first reviewer ($p = 0.008$) and for the second reviewer ($p = 0.012$). Only one patient with skull base osteomyelitis was determined to have a high apparent diffusion coefficient of the skull base by both reviewers who was misdiagnosed as having an uninvolved skull base.

Table 1. Mean apparent diffusion coefficients of skull base in necrotising otitis externa patients with and without skull base osteomyelitis

Reviewer	Necrotising otitis externa with skull base osteomyelitis*	Necrotising otitis externa without skull base involvement†	P-value
1st reviewer	0.851 ± 0.15 (0.72–1.23)	1.065 ± 0.19 (0.73–1.32)	0.008
2nd reviewer	0.841 ± 0.14 (0.74–1.20)	1.045 ± 0.20 (0.73–1.30)	0.012

Data represent mean (± standard deviation) apparent diffusion coefficients (10^{-3}mm^2/s), with ranges in parentheses, unless indicated otherwise. *n = 10; †n = 14
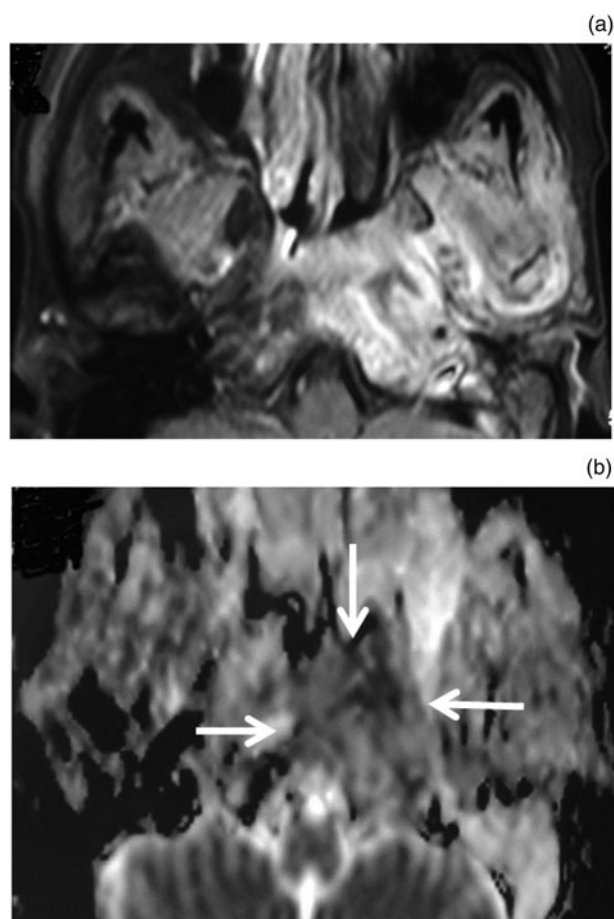

Fig. 2. Necrotising otitis externa without skull base involvement. (a) Axial, contrast-enhanced magnetic resonance imaging scan shows diffuse enhancing lesion infiltrating the left masticator space in a patient with necrotising otitis externa. The lesion extends into the skull base bone marrow on the left side. (b) Apparent diffusion coefficient map shows high apparent diffusion coefficient values for the bony lesion of the skull base (arrows), with calculated apparent diffusion coefficient values of 1.21 and 1.17 ×10^{-3}mm^2/s for each reviewer respectively.

The apparent diffusion coefficients of 0.945 and 0.915 ×10^{-3}mm^2/s were optimal threshold values for predicting skull base osteomyelitis in necrotising otitis externa patients, with area under the curve values of 0.825 and 0.800, accuracy of 87.5 per cent and 83.3 per cent, sensitivity of 85.7 per cent and 90.0 per cent, specificity of 90.0 per cent and 78.6 per cent, positive predictive values of 92.3 per cent and 75.0 per cent, and negative predictive values of 81.8 per cent and 91.7 per cent, for each reviewer respectively (Table 2 and Figure 3).

Discussion

The main finding in this study is that the apparent diffusion coefficient of the skull base can predict skull base osteomyelitis in patients with necrotising otitis externa. There is restricted diffusion with a low apparent diffusion coefficient of the skull base lesion in patients with skull base osteomyelitis, and unrestricted diffusion with a high apparent diffusion coefficient of the skull base in patients with necrotising otitis externa without skull base involvement, with excellent interobserver agreement of the apparent diffusion coefficients by both reviewers.

Previous studies using computed tomography and routine MRI reported that there is a thin line of demarcation between osteitis and osteomyelitis. Differentiation between both entities is crucial because they involve different treatment methods and planning.[12–15] The treatment of osteitis involves antibiotics alone, whereas osteomyelitis must be treated surgically with debridement and sequestrectomy.[27]

Previous studies applied diffusion-weighted imaging in the assessment of infection of the spine, masticator space and diabetic foot.[22,23,28] Diffusion-weighted imaging has the ability to distinguish between acute and chronic inflammatory changes. Only one study investigated the role of diffusion-weighted imaging for monitoring patients with necrotising otitis externa after therapy.[26] That study reported a decrease in the apparent diffusion coefficient value for necrotising otitis externa after a response to the therapy. The apparent diffusion coefficient value facilitated quantitative assessment of the disease activity; hence, this parameter can be helpful for assessing the therapeutic response in subsequent follow-up examinations.[26]

In this study, the mean apparent diffusion coefficient value for the skull base bone marrow in nine patients with skull base osteomyelitis was lower than that in necrotising otitis externa patients without skull base involvement, as determined by two reviewers. The difference in the apparent diffusion coefficient between both entities may be attributed to the different pathological nature of the two conditions. Skull base osteomyelitis is characterised by high cellularity (inflammation and pus cells, dead organisms), decreased diffusion space for the water protons, and, hence, subsequent restricted diffusion and lower apparent diffusion coefficient values. The lower skull base bone marrow diffusion-weighted imaging signal intensity in necrotising otitis externa may be attributed to lower cellularity and consequently higher apparent diffusion coefficient values. These pathological criteria are responsible for the significant difference in the apparent diffusion coefficient values between both entities.[19,23,28,29]

In this study, only one patient with skull base osteomyelitis was determined to have a high apparent diffusion coefficient value for the skull base that was misdiagnosed as non-involvement of the skull base. This may be attributed to the early skull base infection with bone marrow oedema of the skull base, which is associated with more fluid and unrestricted diffusion, with a high apparent diffusion coefficient value for the skull base.[22,23]

Diffusion-weighted imaging can be conducted using either echo-planar imaging or non-echo-planar imaging diffusion-weighted imaging sequences. Echo-planar imaging diffusion-weighted imaging involves scanning a large volume within a short period (1 minute) and has an adequate signal-to-noise

Table 2. Receiver operating characteristic curve results of apparent diffusion coefficients for both reviewers

Reviewer	Threshold value	AUC	Sensitivity (%)	Specificity (%)	PPV (%)	NPV (%)	Accuracy (%)
1st reviewer	0.945	0.825	85.7	90.0	92.3	81.8	87.5
2nd reviewer	0.915	0.800	90.0	78.6	75.0	91.7	83.3

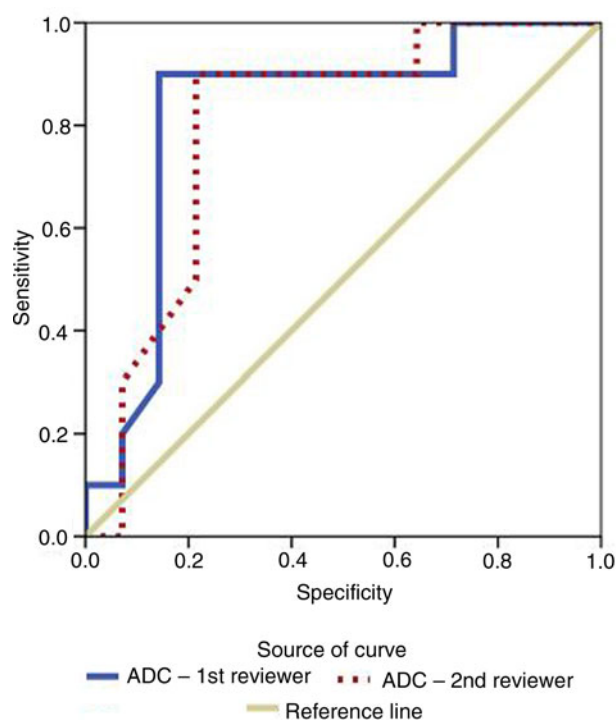AUC = area under the curve; PPV = positive predictive value; NPV = negative predictive value

Fig. 3. Receiver operating characteristic curve. The optimal threshold apparent diffusion coefficient (ADC) used to predict skull base osteomyelitis in patients with necrotising otitis externa was 0.945 ×10^{-3}mm^2/s and 0.915 ×10^{-3}mm^2/s, with an area under the curve of 0.825 and 0.800, accuracy of 87.5 per cent and 83.3 per cent, sensitivity of 85.7 per cent and 90.0 per cent, and specificity of 90.0 per cent and 78.6 per cent for each reviewer respectively.

ratio; however, it is associated with susceptibility and chemical shift artefacts, especially at air–tissue interfaces, although parallel imaging can decrease susceptibility artefacts and image blurring. Non-echo-planar imaging diffusion-weighted imaging has a long echo time, high signal-to-noise ratio and is without susceptibility artefacts or image distortion at air–tissue interfaces such as the skull base; however, it is associated with ghosting artefacts and is more sensitive to motion artefacts.[30–38] Diffusion-weighted imaging of the skull base has been conducted using echo-planar imaging diffusion-weighted imaging[17,35] and non-echo-planar imaging diffusion-weighted imaging.[38] In our study, we employed echo-planar imaging diffusion-weighted imaging using a shorter echo time and a large receiver bandwidth, to reduce the time of dephasing and minimise subsequent signal loss.

This study has a few limitations. First, it was a retrospective study with a small number of patients. Further studies with larger numbers of patients are recommended. Second, this study applied diffusion-weighted imaging; further studies using diffusion tensor imaging combined with dynamic contrast-enhanced MRI and proton magnetic resonance spectroscopy, on a 3 Tesla scanner,[39–46] will improve the results. Third, this study employed echo-planar imaging diffusion-weighted imaging of the skull base, which is associated with susceptibility changes

at air–tissue interfaces that lead to image distortion and artefacts. Further studies that use non-echo-planar imaging diffusion-weighted imaging are recommended, with the application of parallel imaging to decrease the artefacts of diffusion-weighted imaging at the skull base.

- The apparent diffusion coefficient of the skull base is lower in necrotising otitis externa patients with skull base osteomyelitis than in those without skull base involvement
- Apparent diffusion coefficient can be used for predicting skull base osteomyelitis in necrotising otitis externa patients
- The optimal threshold apparent diffusion coefficient values of two reviewers used to predict skull base osteomyelitis in necrotising otitis externa patients were 0.945 and 0.915 ×10^{-3}mm^2/s

Conclusion

Apparent diffusion coefficient is a non-invasive imaging parameter that can be used to predict skull base osteomyelitis in patients with necrotising otitis externa.

Competing interests. None declared

References

1 Peled C, El-Seid S, Bahat-Dinur A, Tzvi-Ran LR, Kraus M, Kaplan D. Necrotizing otitis externa--analysis of 83 cases: clinical findings and course of disease. *Otol Neurotol* 2019;**40**:56–62
2 Cooper T, Hildrew D, McAfee JS, McCall AA, Branstetter BF 4th, Hirsch BE. Imaging in the diagnosis and management of necrotizing otitis externa: a survey of practice patterns. *Otol Neurotol* 2018;**39**:597–601
3 Peled C, Kraus M, Kaplan D. Diagnosis and treatment of necrotising otitis externa and diabetic foot osteomyelitis - similarities and differences. *J Laryngol Otol* 2018;**132**:775–9
4 Hatch JL, Bauschard MJ, Nguyen SA, Lambert PR, Meyer TA, McRackan TR. Malignant otitis externa outcomes: a study of the University HealthSystem Consortium database. *Ann Otol Rhinol Laryngol* 2018;**127**:514–20
5 Khan MA, Quadri SAQ, Kazmi AS, Kwatra V, Ramachandran A, Gustin A et al. A comprehensive review of skull base osteomyelitis: diagnostic and therapeutic challenges among various presentations. *Asian J Neurosurg* 2018;**13**:959–70
6 Ridder GJ, Breunig C, Kaminsky J, Pfeiffer J. Central skull base osteomyelitis: new insights and implications for diagnosis and treatment. *Eur Arch Otorhinolaryngol* 2015;**272**:1269–76
7 Le Clerc N, Verillaud B, Duet M, Guichard JP, Herman P, Kania R. Skull base osteomyelitis: incidence of resistance, morbidity, and treatment strategy. *Laryngoscope* 2014;**124**:2013–16
8 Kornilenko L, Rocka S, Balseris S, Arechvo I. Clinical challenges in the diagnosis and treatment of temporal bone osteomyelitis. *Case Rep Otolaryngol* 2017;**2017**:4097973
9 Chen JC, Yeh CF, Shiao S, Tu TY. Temporal bone osteomyelitis: the relationship with malignant otitis externa, the diagnostic dilemma, and changing trends. *ScientificWorldJournal* 2014;**2014**:591714
10 van Kroonenburgh AMJL, van der Meer WL, Bothof RJP, van Tilburg M, van Tongeren J, Postma AA. Advanced imaging techniques in skull base osteomyelitis due to malignant otitis externa. *Curr Radiol Rep* 2018;**6**:3
11 Adams A, Offiah C. Central skull base osteomyelitis as a complication of necrotising otitis externa: imaging findings, complications, and challenges of diagnosis. *Clin Radiol* 2012;**67**:e7–16
12 Razek AA, Huang BY. Lesions of the petrous apex: classification and findings at CT and MR imaging. *Radiographics* 2012;**32**:151–73

13 Goh JPN, Karandikar A, Loke SC, Tan TY. Skull base osteomyelitis secondary to malignant otitis externa mimicking advanced nasopharyngeal cancer: MR imaging features at initial presentation. *Am J Otolaryngol* 2017;**38**:466–71

14 Lee JE, Song JJ, Oh SH, Chang SO, Kim CH, Lee JH. Prognostic value of extension patterns on follow-up magnetic resonance imaging in patients with necrotizing otitis externa. *Arch Otolaryngol Head Neck Surg* 2011;**137**:688–93

15 Rozenblum-Beddok L, Verillaud B, Paycha F, Vironneau P, Abulizi M, Benada A *et al.* 99mTc-HMPAO-leukocyte scintigraphy for diagnosis and therapy monitoring of skull base osteomyelitis. *Laryngoscope Investig Otolaryngol* 2018;**3**:218–24

16 Abdel Razek AA, Kamal E. Nasopharyngeal carcinoma: correlation of apparent diffusion coefficient value with prognostic parameters. *Radiol Med* 2013;**118**:534–9

17 Abdel Razek A, Mossad A, Ghonim M. Role of diffusion-weighted MR imaging in assessing malignant versus benign skull-base lesions. *Radiol Med* 2011;**116**:125–32

18 Connolly M, Srinivasan A. Diffusion-weighted imaging in head and neck cancer technique, limitations, and applications. *Magn Reson Imaging Clin N Am* 2018;**26**:121–33

19 Abd-El Khalek Abd-ALRazek A, Fahmy DM. Diagnostic value of diffusion-weighted imaging and apparent diffusion coefficient in assessment of the activity of Crohn disease: 1.5 or 3 T. *J Comput Assist Tomogr* 2018;**42**:688–96

20 Schmid-Tannwald C, Schmid-Tannwald CM, Morelli JN, Albert NL, Braunagel M, Trumm C *et al.* The role of diffusion-weighted MRI in assessment of inflammatory bowel disease. *Abdom Radiol* 2016;**41**:1484–94

21 Ozgen B, Oguz KK, Cila A. Diffusion MR imaging features of skull base osteomyelitis compared with skull base malignancy. *AJNR Am J Neuroradiol* 2011;**32**:179–84

22 Daghighi MH, Poureisa M, Safarpour M, Behzadmehr R, Fouladi DF, Meshkini A *et al.* Diffusion-weighted magnetic resonance imaging in differentiating acute infectious spondylitis from degenerative Modic type 1 change; the role of b-value, apparent diffusion coefficient, claw sign and amorphous increased signal. *Br J Radiol* 2016;**89**:20150152

23 Abdel Razek A, Samir S. Diagnostic performance of diffusion-weighted MR imaging in differentiation of diabetic osteoarthropathy and osteomyelitis in diabetic foot. *Eur J Radiol* 2017;**89**:221–5

24 Lingam RK, Bassett P. A meta-analysis on the diagnostic performance of non-echoplanar diffusion-weighted imaging in detecting middle ear cholesteatoma: 10 years on. *Otol Neurotol* 2017;**38**:521–8

25 Razek AAKA. Assessment of masses of the external ear with diffusion-weighted MR imaging. *Otol Neurotol* 2018;**39**:227–31

26 Cherko M, Nash R, Singh A, Lingam RK. Diffusion-weighted magnetic resonance imaging as a novel imaging modality in assessing treatment response in necrotizing otitis externa. *Otol Neurotol* 2016;**37**:704–7

27 Prasad SC, Prasad KC, Kumar A, Thada ND, Rao P, Chalasani S. Osteomyelitis of the temporal bone: terminology, diagnosis, and management. *J Neurol Surg B* 2014;**75**:324–31

28 Abdel Razek AA, Nada N. Role of diffusion-weighted MRI in differentiation of masticator space malignancy from infection. *Dentomaxillofac Radiol* 2013;**42**:20120183

29 Razek AA, Sieza S, Maha B. Assessment of nasal and paranasal sinus masses by diffusion-weighted MR imaging. *J Neuroradiol* 2009;**36**:206–11

30 Razek AA. Diffusion-weighted magnetic resonance imaging of head and neck. *J Comput Assist Tomogr* 2010;**34**:808–15

31 Abdel Razek AA, Soliman N, Elashery R. Apparent diffusion coefficient values of mediastinal masses in children. *Eur J Radiol* 2012;**81**:1311–14

32 Razek AAA. Ashmalla G. Assessment of paraspinal neurogenic tumors with diffusion-weighted MR imaging. *Eur Spine J* 2018;**27**:841–6

33 Surov A, Nagata S, Razek AA, Tirumani SH, Wienke A, Kahn T. Comparison of ADC values in different malignancies of the skeletal musculature: a multicentric analysis. *Skeletal Radiol* 2015;**44**:995–1000

34 Razek AA, Lattif MA, Denewer A, Farouk O, Nada N. Assessment of axillary lymph nodes in patients with breast cancer with diffusion-weighted MR imaging in combination with routine and dynamic contrast MR imaging. *Breast Cancer* 2016;**23**:525–32

35 Guler E, Ozgen B, Mut M, Soylemezoglu F, Oguz KK. The added value of diffusion magnetic resonance imaging in diagnosis and posttreatment evaluation of skull base chordoma. *J Neurol Surg B Skull Base* 2017;**78**:256–65

36 Abdel Razek AAK, Elkhamary SM, Nada N. Correlation of apparent diffusion coefficient with histopathological parameters of salivary gland cancer. *Int J Oral Maxillofac Surg* 2019;**48**:995–1000

37 Razek AAKA. Prediction of malignancy of submandibular gland tumors with apparent diffusion coefficient. *Oral Radiol* 2019;**35**:11–15

38 Soni N, Gupta N, Kumar Y, Mangla M, Mangla R. Role of diffusion-weighted imaging in skull base lesions: a pictorial review. *Neuroradiology J* 2017;**30**:370–84

39 Razek AA, Nada N. Correlation of choline/creatine and apparent diffusion coefficient values with the prognostic parameters of head and neck squamous cell carcinoma. *NMR Biomed* 2016;**29**:483–9

40 Abdel Razek AAK. Routine and advanced diffusion imaging modules of the salivary glands. *Neuroimaging Clin N Am* 2018;**28**:245–54

41 Razek AAKA. Diffusion tensor imaging in differentiation of residual head and neck squamous cell carcinoma from post-radiation changes. *Magn Reson Imaging* 2018;**54**:84–9

42 El-Serougy L, Abdel Razek AA, Ezzat A, Eldawoody H, El-Morsy A. Assessment of diffusion tensor imaging metrics in differentiating low-grade from high-grade gliomas. *Neuroradiol J* 2016;**29**:400–7

43 Abdel Razek AAK. Arterial spin labelling and diffusion-weighted magnetic resonance imaging in differentiation of recurrent head and neck cancer from post-radiation changes. *J Laryngol Otol* 2018;**132**:923–8

44 Razek AA, Gaballa G, Megahed AS, Elmogy E. Time resolved imaging of contrast kinetics (TRICKS) MR angiography of arteriovenous malformations of head and neck. *Eur J Radiol* 2013;**82**:1885–91

45 Abdel Razek AA, Samir S, Ashmalla GA. Characterization of parotid tumors with dynamic susceptibility contrast perfusion-weighted magnetic resonance imaging and diffusion-weighted MR imaging. *J Comput Assist Tomogr* 2017;**41**:131–6

46 Allam H, Abdel Razek A, Ashraf B, Khaled M. Reliability of diffusion-weighted MR imaging in differentiation of recurrent cholesteatoma and granulation tissue after intact canal wall mastoidectomy. *J Laryngol Otol* 2019;**133**:1083–6